Evaluation of Wind Vectors Measured by a Bistatic Doppler Radar Network

KATJA FRIEDRICH AND MARTIN HAGEN

Institut fuer Physik der Atmosphaere, Deutsches Zentrum fuer Luft- und Raumfahrt (DLR), Oberpfaffenhofen, Wessling, Germany

(Manuscript received 10 March 2004, in final form 2 July 2004)

ABSTRACT

By installing and linking additional receivers to a monostatic Doppler radar, several wind components can be measured and combined into a wind vector field. Such a bistatic Doppler radar network was developed in 1993 by the National Center for Atmospheric Research and has been in operation at different research departments. Since then, the accuracy of wind vectors has been investigated mainly based on theoretical examinations. Observational analysis of the accuracy has been limited to comparisons of dual-Doppler-derived wind vectors always including the monostatic Doppler radar. Intercomparisons to independent wind measurements have not yet been accomplished. In order to become an alternative to monostatic multiple–Doppler applications, the reliability of wind vector fields has to be also proven by observational analysis. In this paper wind vectors measured by a bistatic Doppler radar network are evaluated by 1) internally comparing results of bistatic receivers; 2) comparing with independent wind measurements observed by a second Doppler radar; and 3) comparing with in situ flight measurements achieved with a research aircraft during stratiform precipitation events. Investigations show how reliable bistatically measured wind fields are and how they can contribute highly to research studies, weather surveillance, and forecasting. As a result of the intercomparison, the instrumentation error of the bistatic receivers can be assumed to be within 1 m s^{-1}. Differences between bistatic Doppler radar and independent measurements range mainly between 2 and 3 m s^{-1}.

1. Introduction

Three-dimensional wind fields together with high-resolution vertical wind profiles are one of the greatest observational needs for regional mesoscale numerical weather prediction (NWP) and a key nowcasting parameter as proposed by the World Meteorological Organisation's expert team on observational data requirements and redesign of the global observing system in their final report (WMO 2002). Owing to a three-dimensional coverage in space with high temporal and spatial resolution, using weather radar data like Doppler velocity and precipitation is favored, especially for regional NWP and synoptic meteorology.

Since the mid-1950s, when the first systematic observations of weather echoes with Doppler radars were carried out, Doppler techniques have already proven great potential for short-term forecasting, severe weather warning, and aviation meteorology (Rogers 1990). The great progress in understanding weather phenomena and detecting severe weather, like microbursts, prompted most national weather services to deploy a Doppler radar network (Zrnić 1996). At the same time, the usage of multiple-Doppler information has been promoted in order to determine wind vector fields in real time. Brown and Peace (1968) were the first to present wind vectors measured by two radar systems, followed by the pioneering work of Armijo (1969) and Lhermitte (1968) who developed new methods for estimating wind and precipitation velocities. Since then the utilization of multiple-Doppler analysis has increased, up to the Severe Environmental Storms and Mesoscale Experiment (SESAME) using seven Doppler radars. The early findings of the basic work were summarized at a workshop on how to operate multiple-Doppler-radar systems (Carbone et al. 1980).

A more economic alternative to several Doppler radar systems, the so-called bistatic Doppler receivers, were developed especially for meteorological applications in 1993 at the National Center for Atmospheric Research (NCAR) in the United States (Wurman 1994). Bistatic receivers, which are spatially separated from the transmitter, are arranged around a monostatic Doppler radar. The theoretical framework for bistatic radar measurements can be found, for instance, in Wurman et al. (1993), Protat and Zawadzki (1999), de Elia and Zawadzki (2001), Takaya and Nakazato (2002), Satoh and Wurman (2003), and references therein. Network design and operation together with advantages of a bistatic as compared to a monostatic Doppler radar system are exhibited, for instance, in Wurman et al. (1994) and Friedrich and Hagen (2004a).

However, when using a bistatic compared to mon-

Corresponding author address: Dr. Katja Friedrich, NOAA/OAR/ETL, Mail Code R/ET7, 325 Broadway, Boulder, CO 82234.
E-mail: Katja.Friedrich@noaa.gov

ostatic multiple-Doppler-radar system, not only the high costs of purchasing and installing the equipment can be reduced, but the interpolation discrepancies as well, simply owing to the fact that in the bistatic system, all Doppler velocity measurements are carried out simultaneously and combined into a wind vector in real time since the measurements are based on just a single source of illumination (Wurman et al. 1993). Until now bistatic receivers have been used solely for experimental research, like the Cooperative Atmosphere–Surface Exchange Study (CASES-97) in 1997 in Kansas (LeMone et al. 2000), the Improvement of Microphysical Parameterization through Observational Verification Experiment (IMPROVE) in 2001 in Washington State (Stoelinga et al. 2003), and the Vertical Transport and Orography Experiment (VERTIKATOR) in 2002 in southern Germany (Lugauer et al. 2003). Although bistatic receivers have been used for different field experiments by different research groups, bistatically measured wind vectors have barely been evaluated with observations. One reason is that the reference instrument has to cover the same spatial area with a similar temporal and spatial resolution and additionally has to be able to measure within the same weather situation. Those demands in mind, bistatically measured wind fields can be evaluated, for instance, using an independent monostatic Doppler radar system. Wurman (1994) compared wind fields from a bistatic dual-Doppler system with those from a traditional monostatic dual-Doppler network. He demonstrated the ability to retrieve accurate wind fields and shallow surface divergence fields with a bistatic dual-Doppler network during three different weather events. Satoh and Wurman (1999) compared wind vectors derived from three pairs of dual-Doppler analysis in a stratiform weather situation. However, one disadvantage of both investigations is that the wind velocities measured by the monostatic Doppler radar were used to retrieve both bistatically measured and the monostatically measured wind vectors, respectively. Therefore, those comparisons were not achieved using two independent wind measurements. Point measurements such as in situ flight measurements and radiosoundings, on the other hand, cannot provide a spatial coverage but will nevertheless contribute to a reliable evaluation.

In this paper measurements of the bistatic multiple-Doppler-radar network operated by the Deutsches Zentrum für Luft- und Raumfahrt (DLR) in Oberpfaffenhofen (OP), close to Munich in southern Germany, are compared both to those wind measurements achieved by an independent Doppler radar operated by the German Weather Service (DWD) and to wind measurements achieved with the DLR Falcon research aircraft during three stratiform precipitation events (see sections 3 and 4). Before evaluating wind fields, system configuration and evaluation performance, including an error source discussion, are presented in section 2.

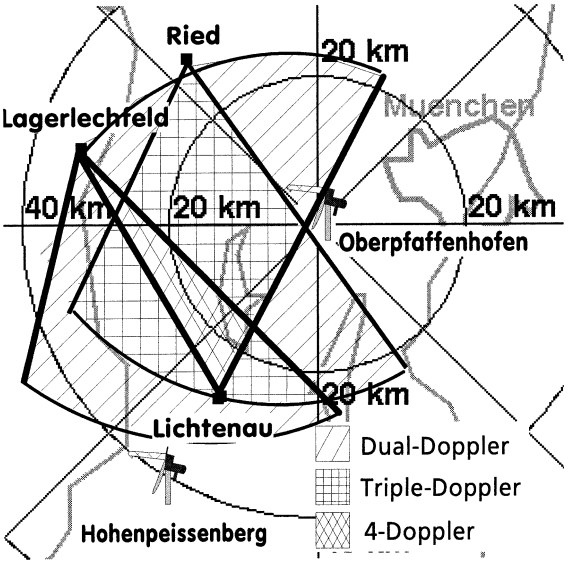

FIG. 1. Map of the bistatic multiple-Doppler-radar network at the DLR in OP consisting of POLDIRAD and three bistatic receivers located at Lichtenau, Lagerlechfeld, and Ried. The investigation area is restricted by horizontal antenna aperture and range resolution. The equation system to calculate the horizontal wind field is exactly determined in the dual-Doppler areas (hatched) and overdetermined in the triple- or quadruple-Doppler areas (cross-hatched). Horizontal wind fields are evaluated with measurements observed by the monostatic Doppler radar located on top of Mount Hohenpeissenberg. More explanations in the text.

2. System configuration and internal evaluation

a. Transceiver and bistatic receiver configuration

The DLR bistatic Doppler radar network consists of the monostatic C-band polarimetric diversity Doppler radar system (POLDIRAD; Schroth et al. 1988) located in OP at 602 m MSL and three bistatic receivers at remote sites each equipped with an antenna and a signal processor. It is the first bistatic radar system operating at C band and with a magnetron transmitter. In Fig. 1 the three bistatic receivers at Lichtenau, at Lagerlechfeld, and at Ried together with the respective viewing angle of the bistatic antenna are illustrated. The investigation area, indicated schematically in Fig. 1, is restricted in range by a variable sample spacing and in azimuthal and vertical direction by the receiving power pattern of the bistatic antennas, which have a horizontal angular aperture covering about 60° and a vertical of about 8°.

With this configuration, the bistatic radar network covers an area of about 50 km × 50 km horizontally and a height up to 5 km within stratiform precipitation. Horizontal wind fields are determined exactly in the dual-Doppler area (hatched area in Fig. 1) and overdetermined in triple-/quadruple-Doppler areas (cross-hatched area in Fig. 1). Due to a limited vertical antenna aperture of 8° oriented close to the ground, the measured wind components are dominated by the horizontal components u and v. As a result, these measurements are

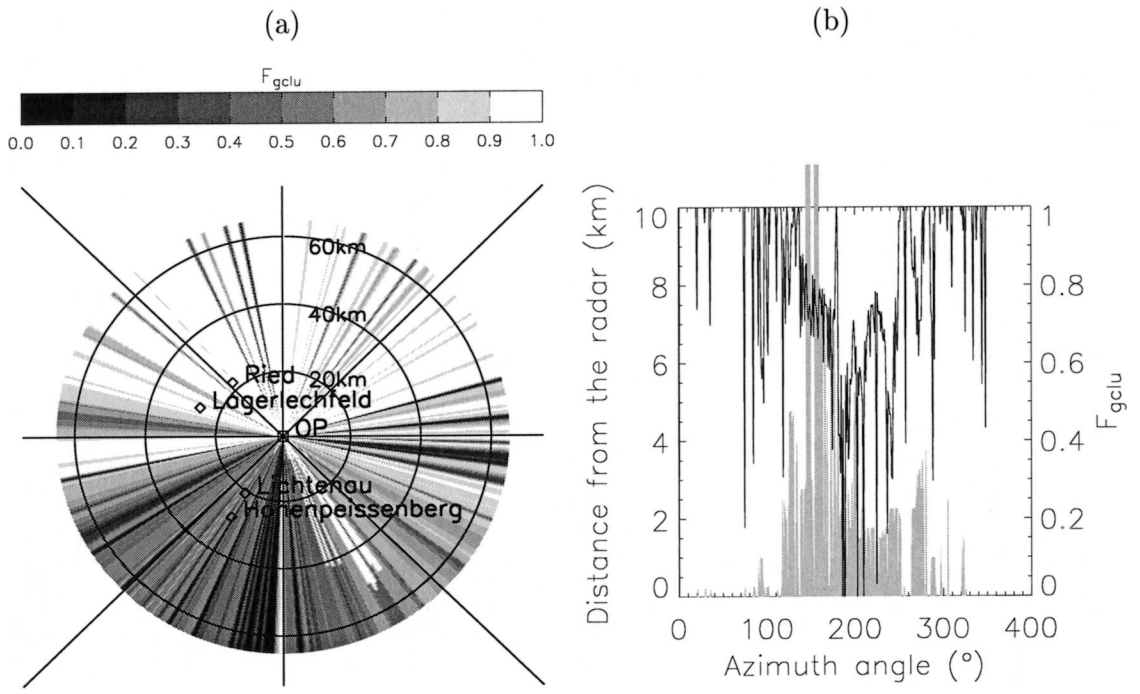

FIG. 2. Beam shielding for POLDIRAD antenna at 1° elevation with a 3-dB beamwidth of 1°. (a) Spatial distribution of the shielding factor, F_{gclu}, ranging from no shielding indicated by 1.0 to total beam blockage assigned by 0.0. (b) Distance of ground clutter from POLDIRAD (gray boxes) and beam shielding factor (solid lines) as a function of azimuth angle.

used only to determine the horizontal wind vector field directly.

b. *Contamination sources and measurement limitations*

Radar measurements can be contaminated by a large number of factors like, for instance, clutter from either normal propagation (permanent clutter) or anomalous propagation of the radiation, biological targets, or chaff. Other acquisition properties, like angular velocity of the rotating antenna, number of averaged pulses, and aliasing effects, also influence the quality of the measured data. For an overview of error sources and solutions the authors refer to other literature, for instance (Alberoni et al. 2002; Meischner 2003).

Especially in mountainous regions, ground clutter contamination is a significant error source for both reflectivity and Doppler velocity. Over the last several years great success has been achieved by detecting and removing ground clutter based on the usage of Doppler velocity information in signal processing. Besides contaminating directly the backscattering signal, ground clutter can totally or partially shield the transmitted radar beam. When beam shielding occurs, reduced peak intensity propagates farther, leading a priori to a reduced backscattering signal. Behind ground clutter, received echos are assigned to a lower height because the main beam is blocked and the backscattering signal comes from the pulse volume edges, which are located at a higher elevation than the main axis of the radar beam. This also holds for Doppler velocity, which is weighted by reflectivity. In the presence of vertical wind shear, the Doppler velocity measured at the pulse volume edge differs from that measured at the beam axis. When 80% of the transmitted beam is shielded, measurements are related only to the upper pulse volume edge, creating a height error, for instance, of about 0.35 km (0.4°) at a distance of 50 km and a 1° beam width. Assuming a vertical wind shear of 10 m s^{-1} $(km)^{-1}$, the resulting velocity error is about 3.5 m s^{-1}.

Figure 2 illustrates beam shielding at 1° elevation around Oberpfaffenhofen for transmitting the POLDIRAD radar beam, which has a vertical beamwidth of 1°. The shielding factor increases linearly between zero for a complete shielding of the 3-dB beamwidth to one for no shielding. The factor is valid for the respective range gate plus for following gates outward along each radial. The calculation is based on a topography dataset that was generated from measurements achieved by the *European Remote Sensing Satellite-2* (*ERS-2*) and has horizontal resolution of 250 m and vertical of 1 m. Topography data were averaged and interpolated onto a polar coordinate centered around POLDIRAD, which samples with an angular resolution of 1° in azimuth and elevation and a radial resolution of 250 m. Measurements using POLDIRAD are strongly contaminated by ground clutter, especially southwest of OP for an elevation of 1°, as shown in Fig. 2a. Figure 2b illustrates the distance of the highest ground clutter value from the

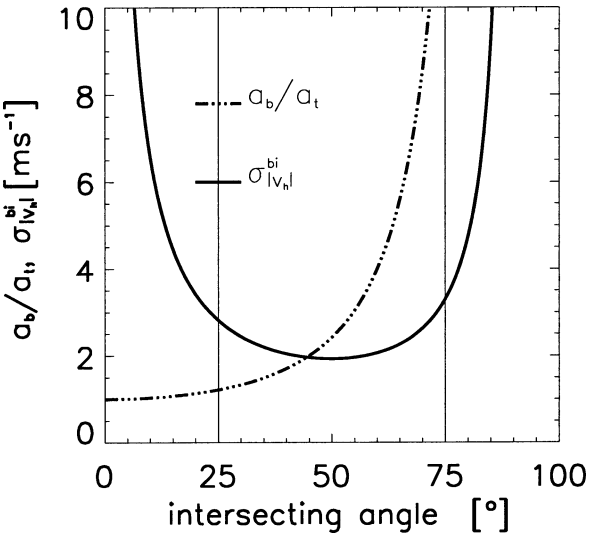

FIG. 3. Dependency of resolution volume length and std dev of the horizontal wind vector, $\boldsymbol{\sigma}_{|v_h|}$, on the intersecting angle β. The resolution volume length for bistatic reception, a_b, is normalized to the constant monostatic resolution volume length, a_t.

radar (gray bars) together with the shielding factor (solid line). Again, high shielding is expected between an azimuth angle of 180° and 247°. Hardly any shielding effects are assumed for elevation angles higher than 1.5° (figures not shown).

When intercomparing radar data, one has to be aware of limits in sensitivity and accuracy. For monostatic radars Doppler velocity measurements have an instrumental error of less than 1 m s^{-1}. In addition to the instrumental error, one has to consider errors caused by the nature of the phenomena under investigation. Turbulence and wind shear, for instance, produce a spread of Doppler velocities around the mean value resulting in higher measurement errors. As the radial distance from the radar increases, there is an increase proportionally of the size of the sample volume and the vertical distance between ground and first radar echo the result of beam broadening and sampling on a spherical coordinate system. Those effects have to be considered when interpolating onto a Cartesian coordinate system. For measurements using a bistatic multiple-Doppler-radar network, accuracy of horizontal wind field determination, range resolution, and size of the investigation area will be summarized shortly in the following.

Both accuracy of the estimated horizontal wind, $\boldsymbol{\sigma}_{|v_h|}$, and spatial resolution of bistatic measurements depend on the intersecting angle[1] between the two measured wind components. The dependency of the two parameters on the intersecting angle, β, and their spatial distribution are illustrated in Figs. 3 and 4. For further

[1] The intersecting angle is the angle between the radial velocity component measured by the monostatic radar and the component perpendicular to the ellipsoid of constant delay measured by the bistatic receiver. Note that it is half of the angle between transmitted and scattered paths.

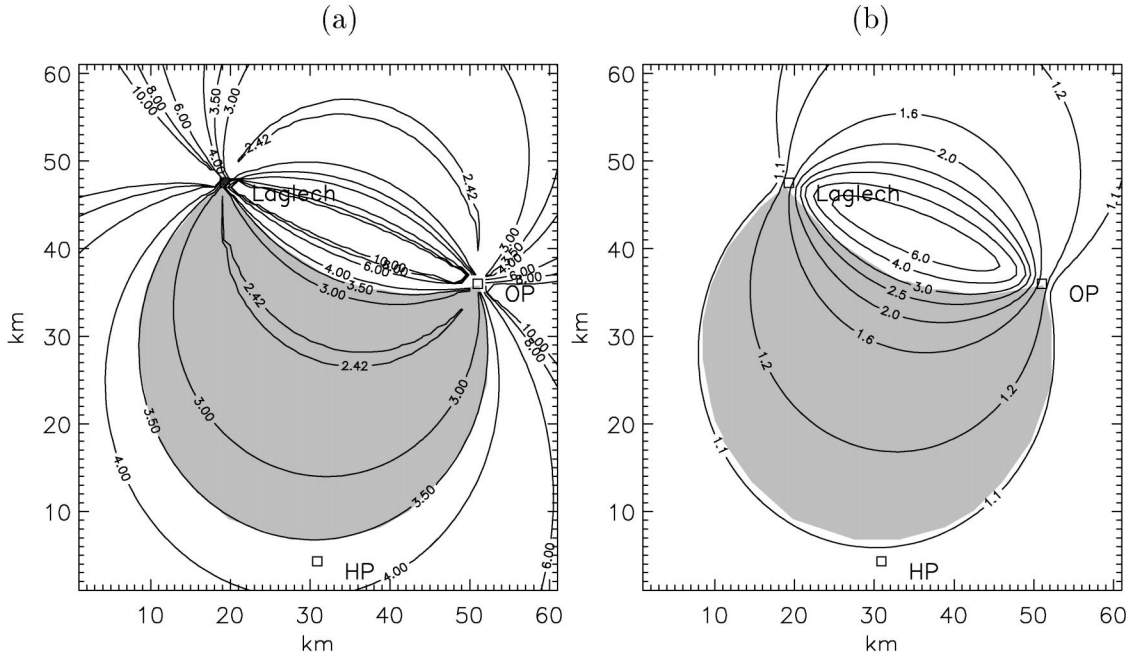

FIG. 4. Spatial distribution of the (a) std dev of the horizontal wind field and (b) resolution volume length normalized by the monostatic resolution volume length at 1.6 km MSL for the bistatic dual-Doppler radar consisting of the receiver at Lagerlechfeld (Laglech) and POLDIRAD at Oberpfaffenhofen (OP). The investigation area of intercomparison with the monostatic Doppler radar at Hohenpeissenberg (HP) is shaded gray. In this area the intersecting angle ranges between 25° and 75°. Note that the maximum contour line is set to a value of 10 in (a) and 6 in (b).

information on wind synthesis of bistatically measured Doppler, the authors refer to Wurman et al. (1993), Protat and Zawadzki (1999), de Elia and Zawadzki (2001), Takaya and Nakazato (2002), Satoh and Wurman (2003), and Friedrich and Caumont (2004). For dual-Doppler analysis, highest accuracy can be achieved when both wind components are perpendicular to each other. In a bistatic network, however, the lowest theoretical standard deviation (std dev) with values of 2.4 m s^{-1} is reached when $\beta = 50°$, as illustrated in Figs. 3 and 4a (Takaya and Nakazato 2002; Satoh and Wurman 2003). Requiring an accuracy of the horizontal wind of less than 3.5 m s^{-1} the target area reduces to an intersecting angle limit of about 25°–75° (cf. Fig. 3 vertical solid lines, Fig. 4a gray marked area). Resolution volume length of bistatic measurements normalized to that of a monostatic radar is illustrated in Fig. 3 (dotted line) and Fig. 4b. Close to the transceiver–receiver baseline, the resolution volume length is considerably larger than the monostatic one. Nevertheless, within the aforementioned intersecting angle limit, one can expect a sufficient spacial resolution.

The area that can be observed by a broad-beam bistatic antenna is restricted by the receiving power pattern. By feeding a weak signal into the bistatic antenna, while an independent microwave receiver measured the beam pattern of the slotted waveguide 180° horizontally as well as at different elevations, the receiving power patterns of bistatic antennas were measured at an antenna test facility at the DLR. The distance between the microwave receiver and the bistatic antenna was about 50 m. As illustrated in Fig. 5a, bistatic antennas used in the DLR bistatic Doppler radar network were designed to receive the main power with a horizontal angular aperture covering ±30° around the principal axis. In the vertical direction, however, the main power is received between 1° and 9°, as illustrated in Fig. 5b. With the sharp power gradient between 0° and 1°, ground-clutter contamination should be suppressed. As a result, measurement can be achieved up to a maximum height of about 4.7–6.2 km at a range from 30 to 40 km with a vertical antenna aperture of about 8°.

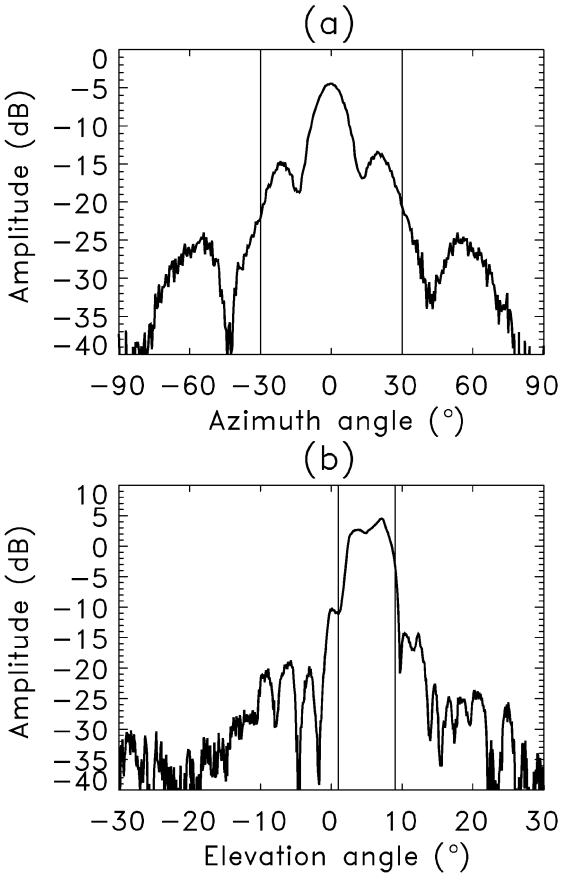

FIG. 5. One-way receiving power pattern (in dB) of vertically polarized bistatic antennas measured in azimuthal direction and for different elevations at a DLR antenna test facility. (a) The receiving power pattern sampled in azimuthal direction for 2.5° elevation. The nominal horizontal angular aperture covering ±30° is indicated by the vertical lines. (b) The receiving power pattern is measured in a vertical direction for an azimuth angle of 0°. The vertical angular aperture covering from 1° to 9° is symbolized by the vertical lines. Note that the 0-dB amplitude level is related to the power fed into the bistatic antenna.

c. Internal evaluation

In order to gain confidence in the performance of bistatic receivers, Doppler velocities of the receivers, included in the DLR bistatic Doppler radar network, are compared to each other. The objective of the internal evaluation is the determination of the instrumental error. For that purpose, two receivers connected to one bistatic antenna were placed at the monostatic radar site in OP so that both receivers measure almost the same velocity component as the monostatic radar system. When using this setup, errors are neglected that can be related to time and space interpolation and to the measurement geometry as proposed, for instance, by Takaya and Nakazato (2002). Doppler velocity measurements were taken during stratiform precipitation with low wind shear and low turbulence characteristics, reducing the appearance of high Doppler velocity variations. Both receivers measured normalized coherent power[2] (NCP) above 0.6, indicating low turbulence for this case. As illustrated in Fig. 6, the majority of data points vary between about ±1 m s^{-1} with a regression line of $y = 1.03x - 0.08$. As a result, the velocity variation of ±1 m s^{-1} is related mainly to the instrumental performance, like the accuracy of the Doppler phase measurement or number of independent echo samples for the time series.

[2] NCP, also known as signal quality index (SQI), is related inversely to the spectral width and ranges from zero to one. It is calculated at the bistatic receivers as NCP $= |R_1|/R_0$, with R_0 and R_1 being the zeroth and first moment of the autocorrelation function taken from the Doppler power spectrum.

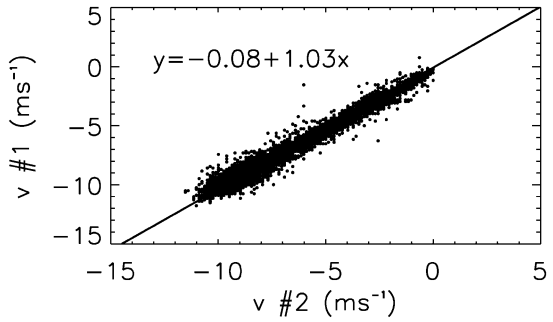

FIG. 6. Scatterplot illustrating Doppler velocities measured by bistatic receivers 1 and 2, both located at OP. The linear regression line and its equation are presented.

3. Intercomparison to monostatic Doppler radar

a. Observation and evaluation procedure

Within the DLR's bistatic Doppler radar network volume scans were performed with a total duration time of about 4 min every 10 min. The vertical spacing for transmitting was chosen to be 1° for an elevation angle 1° to 4° and set to 2° for 4° up to 10° (for case 1) and 18° (for case 2) elevation. The radial wind component of the monostatic C-band Doppler-radar system operated by the Meteorological Observatory Hohenpeissenberg (HP) of the DWD (located 1006 m MSL on top of Mount Hohenpeissenberg) was determined by using data from POLDIRAD and receiver at Lagerlechfeld (Fig. 1). Doppler velocities measured by the DLR system are both dealiased using the four-dimensional dealiasing scheme, 4DD (James and Houze 2001; Friedrich and Caumont 2004), and quality controlled as explained in Friedrich and Hagen (2004b). Data of two successive volume scans are interpolated both to a single reference time (hereafter POLDIRAD reference time), applying a moving frame of reference (Protat and Zawadzki 1999) and onto a Cartesian coordinate system. The latter is achieved using a linear interpolation method based on the usage of a sphere of influence (Protat and Zawadzki 1999). The wind vector is determined based on least squares estimation using the wind information of all available receivers. From this wind vector, the radial wind component as measured by the independent radar is reconstructed. An example of the evaluation performance is given in Fig. 7 for a stratiform precipitation event at 0558 UTC 6 June 2001. First the horizontal wind field is derived using wind information from all available receivers (Fig. 7a) in order to reconstruct the radial velocity component to be measured at the second radar (Fig. 7b). Afterward the Doppler velocity measured at the independent radar site (Fig. 7c) is compared to the reconstructed wind (Fig. 7d). This case is discussed in more detail in section 3c.

To evaluate the bistatically measured multiple-Doppler wind fields, they are compared to radial Doppler velocity fields measured by the HP radar (cf. Fig. 1). The system is included in the DWD radar network, performing operational volume scans every 15 min (Schreiber 1998). The start time of each volume scan is referred to the HP scanning start in the following text. Each volume scan starts at the highest elevation proceeding downward. Doppler data are dealiased using a dual-PRF (pulse repetition frequency) technique and interpolated onto a Cartesian grid using SPRINT software (Mohr et al. 1986).

For the intercomparison both datasets were interpolated onto the same Cartesian coordinate system with a horizontal resolution of 500 m and a vertical of 250 m, leading to a domain height of 4.25 km above radar height (600 m MSL). As discussed in section 2b, the target area was horizontally restricted to a intersecting angle limit between 25° and 75° (cf. Fig. 3) and vertically between 1° and 9° (cf. Fig. 5). Therefore not considered for the intercomparison were those areas of the bistatic Doppler radar network that have large spatial resolution (e.g., close to the transmitter and bistatic receiver baseline, cf. Fig. 3, dashed–dotted line) and low receiving power of the antenna (cf. Fig. 5). An algorithm for correcting beam shielding (Fig. 2) was not applied. The HP scanning start and POLDIRAD reference time together with the statistical analysis of the intercomparison are illustrated in Table 1 for case 1 and in Table 2 for case 2.

b. Stratiform precipitation event, case 1

Illustrating the reliability of bistatic Doppler radar measurements, a weather situation with low wind shear was chosen for the first case study. On 10 April 2001, the trough of a low pressure system centered on the Dutch coast crossed Germany within the course of the morning hours. During noon the occlusion of the vortex reached the observation area with low precipitation and wind shear. Stratiform precipitation with uniform reflectivity was observed between 1200 and 1530 UTC. At ground level a wind-velocity gradient in an east–west direction over a length of 30 km occurred having values of 14 m s^{-1} in the west and 6 m s^{-1} east of the observation area. The mean wind direction was about 260°, varying from 240° to 265°.

Generally, on 10 April 2001 the velocity differences ranged mainly between ± 2 m s^{-1}, in some cases between ± 6 m s^{-1}, with standard deviation values mainly around ± 2 m s^{-1}, as illustrated in Figs. 8 and 9 and in Table 1, respectively. The distribution of the Doppler velocity difference is portrayed for 1322, 1342, 1412, and 1502 UTC at a height level of 2.1 km MSL in Fig. 8. Both systems were able to observe within a variability of ± 2 m s^{-1} 1) main structures such as the wind veering from southwest (Figs. 8a,b) to west/northwest (Figs. 8c,d) or the increase in wind speed at 1342 compared to 1322 UTC (Figs. 8a,b) and 2) finer structures in the wind field such as like local wind shift at 1322 UTC north of HP. While the intercomparison within the inner domain of the target showed differences within

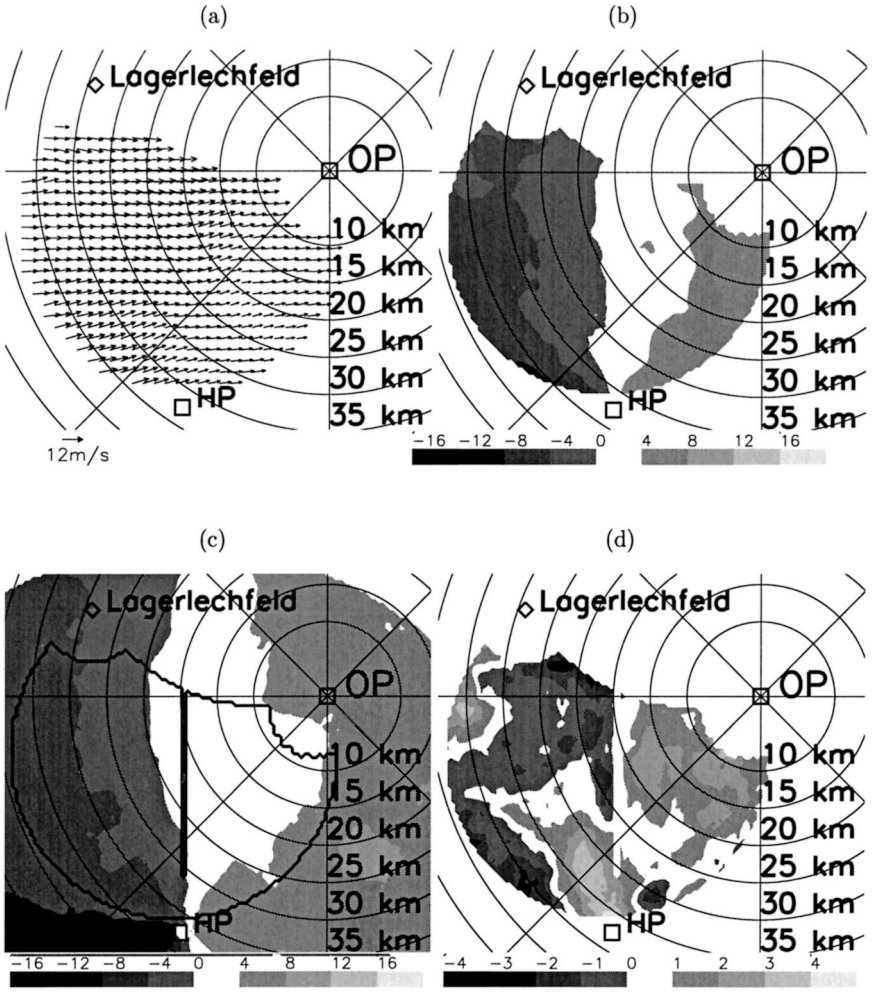

FIG. 7. Example of the evaluation performance illustrating horizontal cross sections at 1.6 km MSL of (a) the horizontal wind (m s^{-1}) using Doppler information from POLDIRAD and the receiver at Lagerlechfeld; (b) the radial velocity of HP reconstructed from (a); (c) the radial velocity (m s^{-1}) measured by HP (grayscale), together with the area of horizontal wind field measurements (thick, solid line); and (d) the velocity difference (m s^{-1}) between (b) and (c) for a stratiform precipitation event at 0558 UTC 6 Jun 2001.

± 2 m s^{-1}, large discrepancies occurred close to the POLDIRAD and HP radars as well as between an azimuth angle related to POLDIRAD ranging between 180° and 212° (Fig. 8). One explanation for the latter effects is the beam shielding of POLDIRAD. As shown in Fig. 2 and discussed in section 2b, the areas between an azimuth of 180° and 250° related to OP is favored by total or a high degree of beam shielding. This explanation is supported when comparing the velocity structure of the measured and reconstructed radial velocity of the HP radar (figure not shown). At the reconstructed radial velocity the zero-velocity isoline formed a bulge between an azimuth angle 210° and 225° at a range from 15 to 25 km. On the other hand, this bulge was less pronounced by the radial velocity measurements taken at the HP radar, which led to a magnitude in the Doppler velocity difference of more than 4 m s^{-1}, as seen in Fig. 8. Radial velocities measured by HP radar were from 4 to 8 m s^{-1} higher than those observed by the bistatic network. This effect was surprisingly observed at those height levels where the main radar beam was not shielded by ground clutter. One can hypothesize that the secondary lobe of the transmitting power pattern hits ground clutter, creating not only a high backscattering echo but having also a zero Doppler-velocity component. Since the total received energy is the sum of all backscattered energy and Doppler velocity is weighted by reflectivity, processed Doppler velocity is reduced due to the zero-Doppler-velocity part coming from the secondary lobe return. High velocity differences close to the radars can be explained by the impact of the vertical velocity component on the measured one. Dual-Doppler analysis close to a monostatic radar system can only be achieved when one radar scans with a

TABLE 1. Statistical analysis of wind field comparison between the bistatic multiple-Doppler radar (denoted as OP) and the Doppler radar system at Hohenpeissenberg (denoted as HP) for 10 Apr 2001. HP scanning time (time HP), POLDIRAD reference time (time OP), number of data samples (N), mean values of the Doppler velocity differences, standard deviation (std dev), and correlation coefficient (cc) of the velocity difference are illustrated.

Time HP (UTC)	Time OP (UTC)	N	Mean (m s^{-1})	Std dev (m s^{-1})	cc
1300–1311	1312	31 689	−0.65	1.90	0.951
1315–1326	1322	35 081	−0.46	1.99	0.947
1330–1341	1332	40 797	−0.04	2.28	0.954
1330–1341	1342	42 465	−0.62	1.99	0.972
1345–1356	1352	38 022	−0.40	2.25	0.949
1400–1411	1412	29 449	−0.75	1.78	0.964
1415–1426	1422	23 523	−0.39	1.75	0.970
1430–1441	1432	23 301	0.32	2.10	0.958
1430–1441	1442	27 832	−0.02	1.67	0.963
1445–1456	1452	35 210	−0.22	2.19	0.963
1500–1511	1502	35 974	0.04	2.12	0.964
1500–1511	1512	22 421	−0.16	2.51	0.963
1515–1526	1522	29 421	−0.05	2.44	0.951
1530–1541	1527	20 085	1.25	3.12	0.910

TABLE 2. As in Table 1 but for 6 Jun 2001.

Time HP (UTC)	Time OP (UTC)	N	Mean (m s^{-1})	Std dev (m s^{-1})	cc
0600–0611	0603	42 956	0.38	1.23	0.970
0600–0611	0613	46 404	0.44	1.44	0.962
0615–0626	0623	46 546	0.44	1.36	0.960
0630–0641	0633	46 379	0.66	1.64	0.945
0630–0641	0643	45 935	0.29	1.55	0.951
0645–0656	0653	45 818	0.58	1.34	0.962
0700–0711	0703	45 943	0.86	1.42	0.961
0700–0711	0713	46 012	0.41	1.44	0.957
0715–0727	0723	46 223	0.53	1.70	0.948
0730–0741	0733	46 206	0.70	1.90	0.939
0730–0741	0743	46 119	−0.09	1.60	0.958
0745–0756	0753	46 082	0.17	1.99	0.933
0815–0826	0832	41 171	−0.04	2.34	0.917
0830–0841	0832	44 465	0.59	2.30	0.924
0830–0841	0842	37 532	0.32	2.14	0.935
0845–0856	0852	35 970	1.30	2.70	0.880
0900–0911	0902	36 710	0.65	2.28	0.922
0900–0911	0911	33 165	0.72	2.07	0.932
0915–0926	0911	24 375	0.86	2.13	0.918
0915–0926	0919	10 740	0.73	1.88	0.854

higher elevation angle than the other one. As a result, the impact of the vertical wind component, therefore the particle fall velocity, on the measured radial component is higher close to the radar than at greater distances. In this case Doppler velocities that are mainly measured in the horizontal direction are compared with those measured in the vertical direction.

A direct comparison of each Doppler velocity measurement, illustrated by scatterplots in Fig. 9, supported the agreement of Doppler velocities ranging within an interval of ± 2 m s^{-1}. The differences in the magnitude of the velocity are within the margin of instrumental error for Doppler velocity measurements using a bistatic receiver. Furthermore, errors of about ± 2 m s^{-1} are also associated for traditional monostatic dual-Doppler estimations. Nevertheless, the bistatic multiple-Doppler radar system observed lower magnitudes of Doppler velocities than the HP radar, which is indicated by negative velocity differences in Table 1 and Fig. 9. This can result from instrumentation discrepancies, interpolation problems, the domination of beam-shielding effects, or the different observation times. The statistical analysis of the Doppler velocity (Table 1) showed velocity differences that lie mainly below 2.5 m s^{-1} with a maximum standard deviation of 3 m s^{-1}. Mean velocity differences were mainly negative with values close to zero. Note that the time difference between the observations can range from 4 up to 10 min. The correlation coefficient between the bistatically measured and HP-measured Doppler velocities was above 0.9 on 10 April 2001 (cf. Table 1).

In order to quantify the error of the Doppler velocity difference within the three-dimensional volume the cumulative probability distribution function (CDF) was calculated illustrating the percentage of data that lies within a respective velocity difference interval, ε. Figure 12a illustrates the CDF value for each observation time between 1312 and 1527 UTC. As a result, on 10 April 2001, 65% of the velocity differences lay within an interval of 2 m s^{-1}, while the majority reaches even 70%. For $\epsilon = 3$ m s^{-1}, 80% of the differences reached this limit, while again the majority reached even 85%. Investigations on CDF comparing wind components measured solely by the DLR's bistatic network showed within low-wind-shear cases that the velocity difference was about 1 m s^{-1} at CDF $>$ 90% (Friedrich and Caumont 2004). Monitoring high-wind-shear events, the CDF was reduced to around 80% for a velocity difference of 1 m s^{-1}. Note that the CDF is also a main parameter for the intern check procedure included in the quality control scheme for multiple-Doppler-derived horizontal wind fields [a detailed description of the quality control scheme can be found in Friedrich and Hagen (2004b)].

c. Stratiform precipitation event, case 2

In the second case, a cold front passage was monitored passing the investigation area in the morning hours between 0600 and 0900 UTC on 6 June 2001. In the first hour prefrontal winds from the southwest and west dominated. After the frontal system propagated through the investigation area from northwest to southeast between about 0700 and 0800 UTC, wind vectors increased and veered to northwest (Fig. 10). Northwesterly winds were observed until the precipitation passed the investigation area at about 0930 UTC. The wind velocity at ground level varied between 10 and 12 m s^{-1} and increased up to 20 m s^{-1} after frontal passage. Generally, wind shear, in both direction and velocity, was much higher on 6 June than compared to wind fields observed on 10 April 2001.

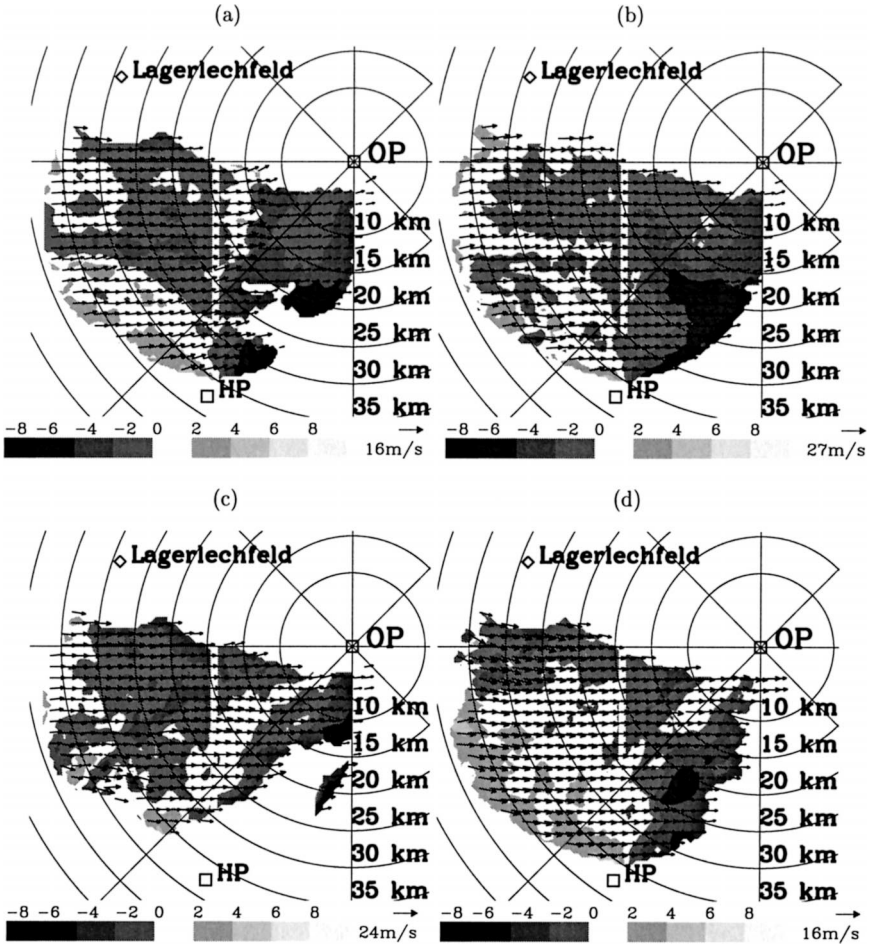

FIG. 8. Horizontal cross section of the velocity difference between the bistatically measured subtracted from the radial velocity observed by radar HP at 2.1 km MSL. The wind vector field (arrows) measured by POLDIRAD at OP and receiver Lagerlechfeld is overlaid. Data were sampled at (a) 1322, (b) 1342, (c) 1412, and (d) 1502 UTC 10 Apr 2001. For clarity every fourth wind vector is displayed.

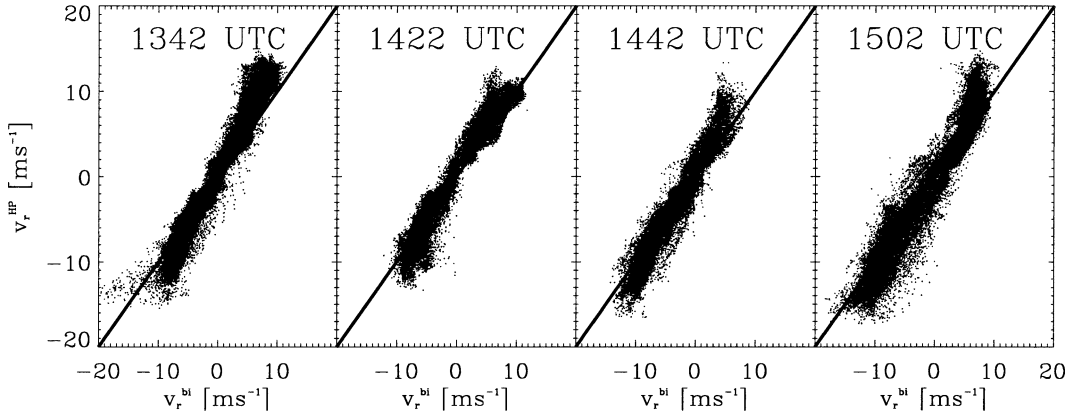

FIG. 9. Scatterplot illustrating the difference between the reconstructed radial velocity (v_r^{bi}) and Doppler velocity measured by the radar HP (v_r^{HP}) at 1342, 1422, 1442, and 1502 UTC 10 Apr 2001.

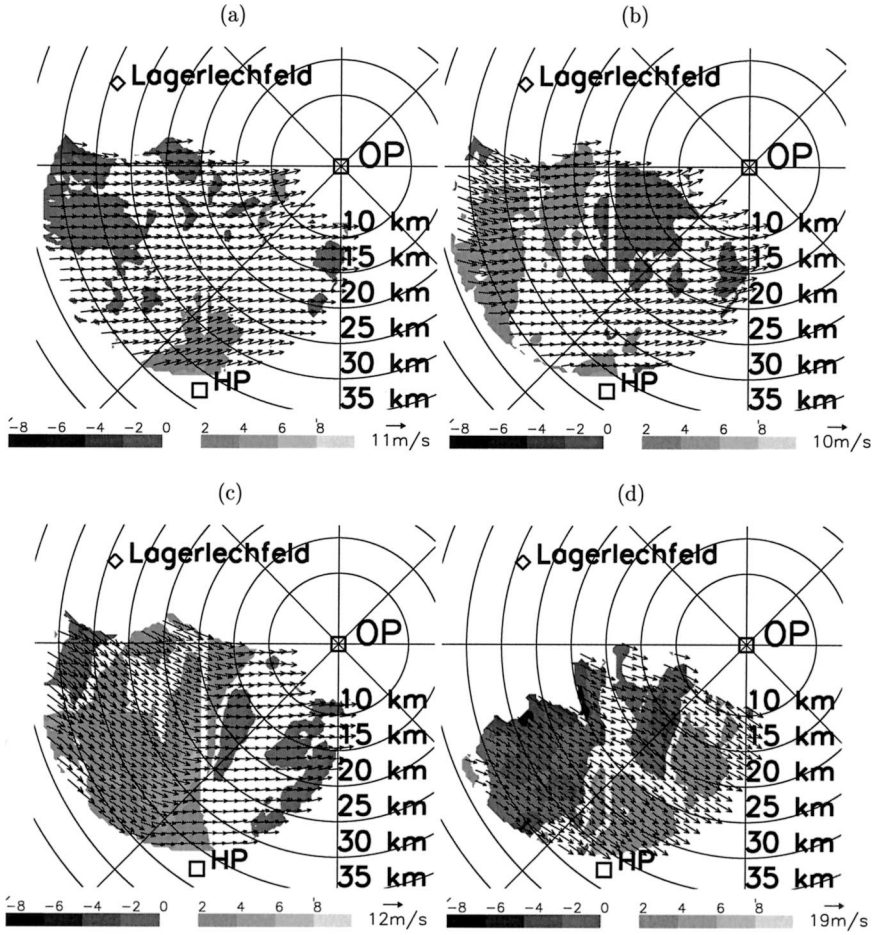

FIG. 10. As in Fig. 8 but for (a) 0613, (b) 0703, (c) 0733, and (d) 0902 UTC 6 Jun 2001. Horizontal cross section was set to 2.1 km MSL.

A selection of the Doppler velocity intercomparison together with the wind vector measured by the bistatic multiple-Doppler system is portrayed in Fig. 10 for four observation times (0613, 0703, 0733, and 0902 UTC). The complete cycle of the frontal passage is displayed with 1) prefrontal winds coming from the west or southwest (Figs. 10a,b); 2) the frontal passage itself with an increase in wind speed and variable wind directions from west and southwest changing to northwest (Fig. 10c); and 3) postfrontal northwesterly winds (Fig. 10d).

The majority of velocity differences lay within a margin of ± 2 m s^{-1} but increased to some extent up to values of even ± 8 m s^{-1}. Nevertheless, Doppler velocity differences were more variable and higher in this case than on 10 April 2001 (cf. Figs. 9, 11). Beam shielding effects, however, were not visible on 6 June 2001, which can be related to the prevailing wind direction and speed. When northwest winds are observed by the POLDIRAD and HP radars, the zero-velocity isoline is oriented in a southwest to northeast direction, that is, along the baseline between the two radars. As a result, one can disregard the impact of the zero velocity components arising from the secondary lobe. The impact on the velocity magnitude is also smaller for low Doppler velocities than for high wind speed. Both effects caused lower Doppler velocity discrepancies in the area of high beam shielding during early hours observing lower velocities and after frontal passage with northwest winds.

Huge discrepancies with absolute velocity differences greater than 4 m s^{-1} measured by the bistatic system compared to the HP radar were noticeable west-southwest of OP at a range of 20–40 km (Fig. 10d). In this area the velocity vector is much higher than in the remaining observation areas. According to the wind vector field, both wind direction change and wind velocity increase occurred rapidly. Different scanning times of each system (both start time and scan strategy) can result in large velocity differences.

Variance of the Doppler velocity differences increased with time, as portrayed in Fig. 11. One can relate the effects to changes in wind direction and velocity during the frontal passage. While at 0623 UTC positive values of the Doppler velocity difference related to

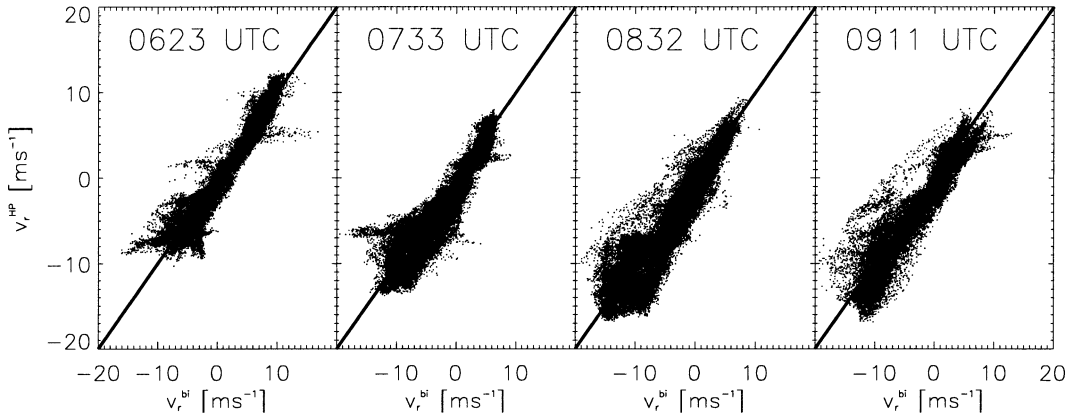

FIG. 11. As Fig. 9 but for POLDIRAD reference times 0623, 0733, 0832, and 0911 UTC 6 Jun 2001.

southwesterly winds (velocities toward the HP radar) dominated the area, the Doppler velocity differences between 0733 and 0911 UTC were negative related to northwesterly winds (velocities away from the HP radar). At the same time the variance increased, especially in the area of negative Doppler velocity differences. During the whole intercomparison period, high variances correlated with high Doppler velocities.

However, the frontal passage itself was well covered by both systems. After the wind vector finally veered to northwest (0911 UTC), variance decreased slightly, as illustrated in Fig. 11. Unfortunately, the precipitation moved farther to the southeast and passed the observation area at about 0930 UTC (as shown in Table 2, column *N*, number of data points). The increase of Doppler velocity variance during frontal passage was also investigated in the statistical analysis (Table 2). The standard deviation increased between 0603 and 0852 UTC and decreased after the wind vector within the observation area veered to northwest. The same effect was investigated using the correlation coefficient.

However, both statistical analysis (Table 2) and scatterplots (Fig. 11) show no clear indication that the bistatic Doppler radar network measures generally lower Doppler velocities compared to the HP radar, as investigated in case 1 (section 3b). The variability within the volume scan increased with time when comparing measurements at 0623 with those at 0911 UTC in Fig. 11. Both the increasing variance with time and a higher variability compared to 10 April 2001 are illustrated in Fig. 12b. About 70% of the differences lay within 2 m s^{-1} for the intercomparison period between 0600 and 0800 UTC. During the entire observation period, 70% of the differences are lower than 2.8 m s^{-1}. The worst

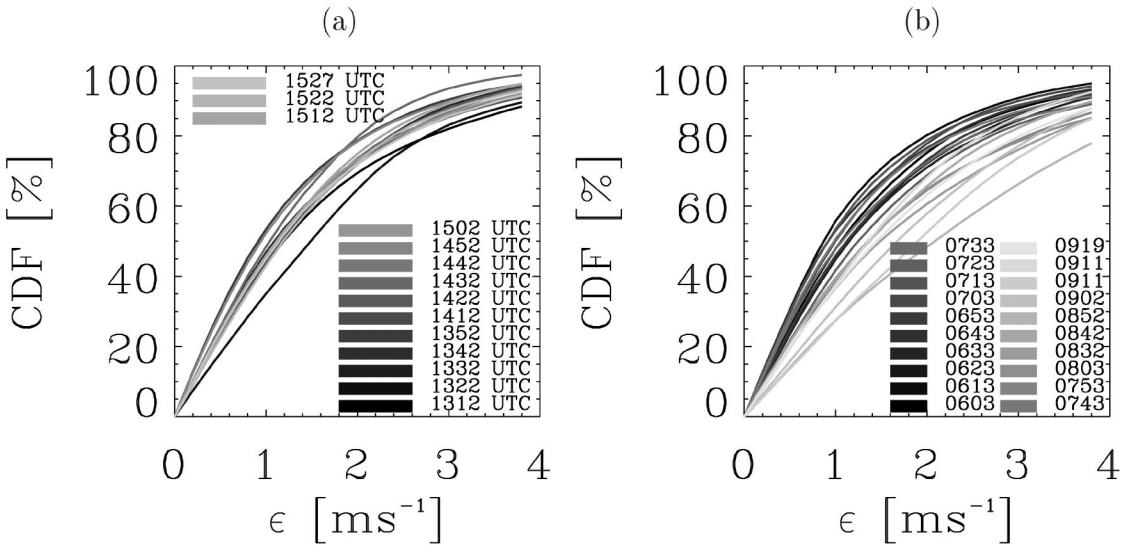

FIG. 12. Comparison between Doppler velocity measured by the DLR's bistatic multiple-Doppler radar network and those observed by the DWD's Doppler radar at Hohenpeissenberg. The cumulative probability distribution function (CDF) of the Doppler velocity differences ϵ is illustrated for a stratiform precipitation event (a) between 1312 and 1527 UTC 10 Apr and (b) between 0603 and 0919 UTC 6 Jun 2001.

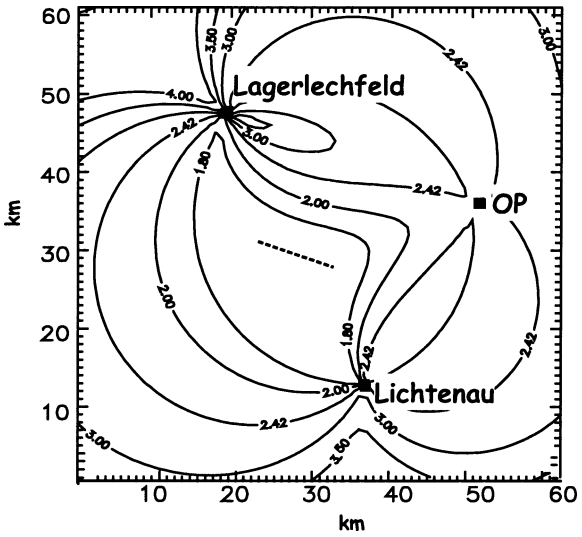

FIG. 13. Spatial distribution of the theoretical std dev of the horizontal wind field normalized by 1 m s^{-1} at 1.8 km MSL for the bistatic dual-Doppler radar consisting of receivers at Lagerlechfeld and Lichtenau and POLDIRAD at Oberpfaffenhofen (OP). The flight path of the aircraft is marked with a dashed line.

agreement was observed at 0852 UTC where a CDF of 70% was reached for 3.2 m s^{-1}.

4. Intercomparison to in situ flight measurement

In situ flight measurements taken on 11 April 2001 were used as an additional independent measurement to evaluate horizontal wind fields determined by the bistatic Doppler radar network. The in situ measurements were performed with the DLR Falcon research aircraft. The wind speed at the position of the aircraft, measured by a five-hole gust probe on the tip of the nose boom, was derived from the differential and the static pressure at the five holes of the half-spherical probe tip. The wind components, u, v, w, in an earth-fixed coordinate system, were derived from the differences between the airflow at the probe, velocity of the aircraft, and orientation of the sensor relative to the ground, which was given by an inertial reference system (IRS). The absolute accuracy of the mean horizontal components is ± 1 m s^{-1} for the aircraft measurements [for more detail, see Boegel and Baumann (1991) and Quante et al. (1996)]. For bistatic dual-Doppler measurements, however, the error in the horizontal wind field determination is less than ± 2 m s^{-1} (dashed line in Fig. 13 represents the flight path).

The aircraft passed the investigation area flying between 1014:15 and 1015:15 UTC from southeast to northwest at an altitude of 1.8 km MSL. Figure 14 exhibits the flight path through the investigation area. The respective elements of UTC time and altitude are labeled. The sensor signals were recorded with 100 Hz corresponding to a sampling interval of typically 1.5 m. The measured data were averaged to an interval of 1 s, which represents a length of about 150 m when the aircraft flies at a speed of about 300 kt. The radar measurements were interpolated from an elliptical coordinate system with the bistatic receiver and POLDIRAD as foci onto a spherical coordinate system centered at POLDIRAD with a resolution volume length of 150 m.

In situ flight measurements of u, v were compared to the velocity components determined by the bistatic multiple-Doppler radar network at 2° and 4° elevation (sampled between 1012:29–1012:32 and 1013:09–1013:11 UTC, respectively). The horizontal wind vector was estimated in spherical coordinates at 2° and 4° elevation from the Doppler velocities measured by POLDIRAD and receivers at Lichtenau and at Lagerlechfeld. The horizontal wind vector field at 4° elevation underlaid by its south wind component of each sample volume is illustrated in Fig. 14.

At 2° elevation, the observation height varied between 1.30 km (at a range of 19 km from OP) and 1.44 km MSL (at a range of 24 km from OP), while at 4° elevation it ranged between 2.0 km (at a range of 19 km from OP) and 2.3 km MSL (at a range of 24 km from OP). The flight path was located at a height of 1.8 km MSL. The west and south wind components, measured by the radar at each aircraft sample point, were interpolated vertically. Note that at a distance of 20 km from the radar, the sample volume of the monostatic radar had a diameter of about 300 m and a length of 150 m (with a 1° antenna beamwidth and a 1-μs pulse length). Therefore, the spatial resolution of the aircraft measurements was higher than that achieved by the radar. An interpolation in time of both datasets was not performed due to a lack of synchronization between time measurements in the aircraft and at the radar. Furthermore, coupled GPS and IRS measurements achieved the positioning of the aircraft with an error ranging from 100 to 200 m per 2–3 min. The error results mainly from the IRS measurements.

Figure 15a illustrates time series of the west and south wind components when measured by the bistatic Doppler radar network and by the in situ instruments. The differences of u, v between the radar and in situ measurements are presented in Fig. 15b. The magnitude of the horizontal wind components measured by the aircraft were mostly 1–2 m s^{-1} higher than the radar measurements and are therefore within the margin of theoretical error for horizontal wind field estimation using a bistatic Doppler radar network. As a result, this comparison shows an agreement within 2 m s^{-1}, which was theoretically expected. Furthermore, the Doppler velocity measurements are in good agreement even with in situ measurements, which are a better ground truth than dual-Doppler estimation since only a time interpolation has to be applied.

Differences in the horizontal wind-field components can be related mainly to the low values of u, v when compared to the absolute error of the velocity measurement. Due to a low temporal evolution of this sys-

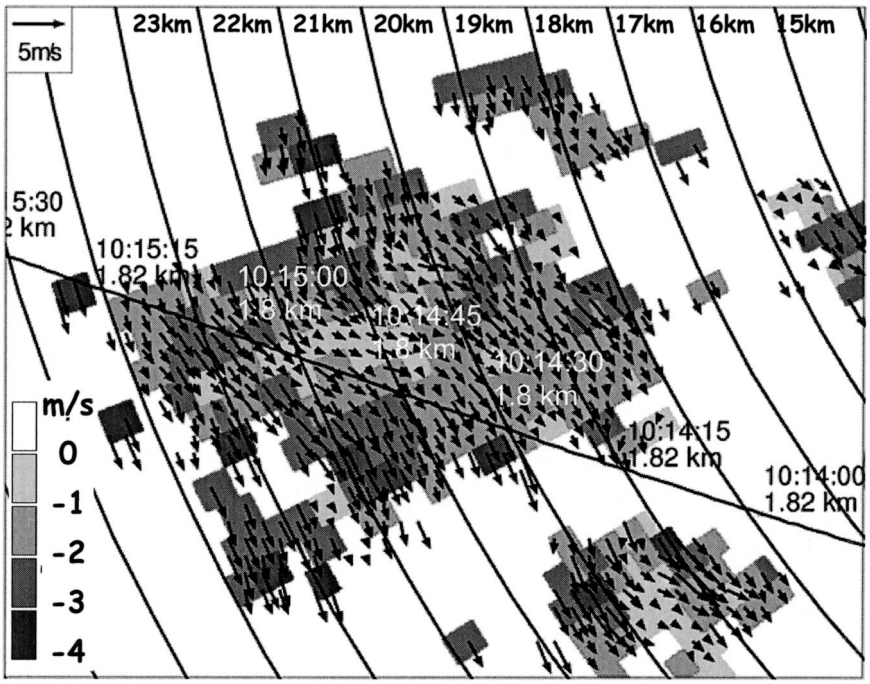

FIG. 14. PPI of the south wind component (in m s^{-1}) (shading) at 4° elevation taken between 1013:09 and 1013:11 UTC 11 Apr 2001, overlaid by the fight path of the aircraft (solid line) and the horizontal wind vector field (arrows). Labels on the fight path indicate time (HH:MM:SS) and altitude MSL. Wind vectors were determined from the Doppler velocities measured by the receivers at Lichtenau and Lagerlechfeld and by POLDIRAD. PPI is centered around POLDIRAD.

tem, having weak precipitation and low wind velocity, the impact of the temporal displacement between the aircraft and radar measurements can be neglected.

For a broader evaluation, flight measurements have to be obtained over a longer time period, a larger spatial coverage, and in various weather situations, for example, with higher wind shear or with higher wind velocities.

5. Concluding remarks

Intercomparing measurements achieved by two different instruments requires an extensive knowledge of error sources that contaminate the measurements. Unfortunately, one is mostly not even able to estimate qualitatively and quantitatively the impact of contamination on the measurement. Since instrumentation limits and error sources can only be partially corrected, one has to keep in mind that the reference instrument does not measure a priori correct winds. As long as all error sources cannot be identified explicitly, one cannot conclude that monostatically measured data are without measurement errors. The question to be answered is now how great is the error on Doppler velocity measurement and how variable is this margin in time and space during the observed weather situation.

Since the first measurements using bistatic receivers were published, the literature has been dominated by discussions on measurement accuracy or contamination sources, such as sidelobe contamination. The impression arose that wind measurements using bistatic receivers are afflicted with large errors or they are even impossible. This paper does not controvert those investigations but shows how bistatically measured wind fields are evaluated and can contribute significantly, for instance during a frontal passage, to research studies, weather surveillance, and forecasting.

Comparing direct measurements of two bistatic receivers, Doppler velocities agree within ± 1 m s^{-1}, which lies within the margin of error for instrumentation accuracy. The Doppler velocity variation is mainly assigned the instrumental error due to the setup of receivers and meteorological conditions. Note that an agreement within about ± 1 m s^{-1} is also assumed for monostatic Doppler radar systems. However, the evaluation of bistatically measured wind fields with both an independent Doppler radar and in situ aircraft measurements also showed reliable results. The magnitude in Doppler velocity differences ranged mainly in all three case studies between 2 and 3 m s^{-1}. The main measurement error within a bistatic network consists generally of an instrumental error, error related to the measurement geometry, and error due to the nature of the phenomena under investigation. While the first two error sources result in a theoretical error ranging between 2 and 3 m s^{-1} [see Fig. 3 of Takaya and Nakazato (2002); Satoh and Wurman (2003)], the meteorologi-

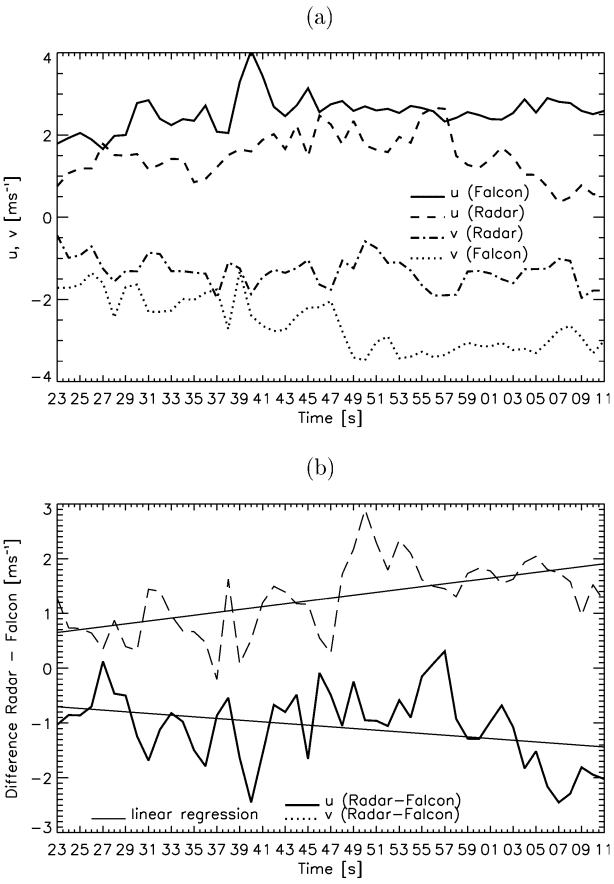

FIG. 15. (a) The values of u, v and (b) its differences (in m s^{-1}) achieved during in situ fight measurements (denoted as Falcon) and measured by the bistatic Doppler radar (denoted as Radar) along the flight path for a stratiform precipitation case on 11 Apr 2001. The aircraft passed the observation area between 1014:23 and 1015:11 UTC. For the west wind component, u, the linear regression line is given by $y = -0.015x + 0.68$, while for the south wind component, v, it is $y = 0.026x + 0.65$.

cally induced variation is hard to quantify. Figure 11 illustrates that meteorological effects influence the error variation to a much higher degree than instrumental effects, albeit one has to link the differences also to discrepancies in the time and space interpolation. Nevertheless, over the years error sources influencing monostatic Doppler radar measurements have been analyzed. Those findings can be applied to bistatic measurements mainly in the same way. Additionally, the quality of bistatic measurements depends strongly on the amount of sidelobe contamination and the time and phase synchronization stability between the transmitter and each receiving source. Synchronization can be monitored by transmitting each receiver's time and phase measurement information to the main hub computer. An alternative to this approach is the comparison of Doppler velocities within areas where the equation system to determine a wind vector field is overdetermined as demonstrated, for instance, by Satoh and Wurman (2003) and Friedrich and Hagen (2004b). In this intercomparison study, receivers not synchronized during the observation time were neglected. Monitoring the amount of sidelobe contamination on the bistatically measured data resulting from the transmitted power pattern is a more sophisticated task [for more details, the authors refer to de Elia and Zawadzki (2000)]. In order to monitor the amount of contamination de Elia and Zawadzki suggested calculating a sidelobe contamination index. Nevertheless, sidelobe contamination has not influenced significantly the radar measurements chosen for this case study since the reflectivity factor was low and on the order of 35 dBZ.

The CDF values range between 65% and 80% for 2 m s^{-1} Doppler velocity differences and 82% and 94% for 3 m s^{-1} on 10 April 2001. During the frontal passage on 6 June 2001, Doppler velocity differences are much greater with CDF values varying between 48% and 80% for 2 m s^{-1} and 67% and 90% for 3 m s^{-1}. Systematic errors in velocity measurement using bistatic receivers were not found on 6 June 2001, although differences higher than 4 m s^{-1} appeared in some areas. Since the instrumental error is about 1 m s^{-1}, large differences are ascribed to the aforementioned meteorological effects.

The authors assume that the gross differences in wind velocity are mainly ascribed to ground clutter contamination and interpolation discrepancies including different scanning strategies. Investigation showed an unexpected large impact of ground clutter on the received power pattern, and therefore on Doppler velocity measurements, which is not necessarily visible as Doppler velocity or reflectivity images. The amount of ground clutter contamination depends on both wind direction and speed; that is, in areas where the radial velocities are small the impact is less pronounced than in areas with high radial velocity measurements.

The comparison of bistatic Doppler radar measurements with another independent instrument, the in situ flight measurement, confirm those results achieved using a monostatic Doppler radar. Again, differences in Doppler velocities are within ± 2 m s^{-1}.

Weather events like, for instance, a frontal passage can be well monitored by a bistatic multiple-Doppler radar network, as shown on 6 June 2001. One of the great advantages of bistatic network is the real-time display of wind vectors, which allows a rapid and easy detection of signatures in the wind field, especially for users with little or no experience in interpreting Doppler velocities.

Acknowledgments. First the authors would like to thank Dr. Jörg Seltmann (German Weather Service, Hohenpeissenberg), together with all members of the DWD radar group, for data acquisition. We greatly benefited from the long and fruitful cooperation with the DWD. We also thank Robert Baumann (DLR) for providing aircraft measurements. We would like to thank

Hermann Scheffold and Lothar Oswald for their technical support and Edgar Clemens for measuring the beam pattern of the bistatic antennas. We are very grateful to Dr. Joshua Wurman and the anonymous reviewer for their precise and useful comments.

REFERENCES

Alberoni, P. P., and Coauthors, 2002: Quality and assimilation of radar data for NWP—A review. COST-717 Working Doc. EUR 20600. [Available online at http://www.smhi.se/cost717.]

Armijo, L., 1969: A theory for the determination of wind and precipitation velocities with Doppler radars. *J. Atmos. Sci.,* **26,** 570–573.

Boegel, W., and R. Baumann, 1991: Test and calibration of the DLR Falcon wind measuring system by maneuvers. *J. Atmos. Oceanic Technol.,* **8,** 5–18.

Brown, R. A., and R. L. Peace, 1968: Mesoanalysis of convective storm utilizing observations from two Doppler radars. Preprints, *13th Conf. on Radar Meteorology,* Montreal, QC, Canada, Amer. Meteor. Soc., 7–14.

Carbone, R. E., and Coauthors, 1980: The multiple Doppler radar workshop, November 1979. *Bull. Amer. Meteor. Soc.,* **61,** 1169–1203.

de Elia, R., and I. Zawadzki, 2000: Sidelobe contamination in bistatic radars. *J. Atmos. Oceanic Technol.,* **17,** 1313–1329.

——, and ——, 2001: Optimal layout of a bistatic radar network. *J. Atmos. Oceanic Technol.,* **18,** 1184–1194.

Friedrich, K., and O. Caumont, 2004: Dealiasing Doppler velocity measured by a bistatic radar network. *J. Atmos. Oceanic Technol.,* **21,** 717–729.

——, and M. Hagen, 2004a: On the use of advanced Doppler radar techniques to determine horizontal wind fields for operational weather surveillance. *Meteor. Appl.,* **11,** 155–171.

——, and ——, 2004b: Wind synthesis and quality control of multiple-Doppler-derived horizontal wind-fields. *J. Appl. Meteor.,* **43,** 38–57.

James, C. N., and R. A. Houze, 2001: A real-time four-dimensional Doppler dealiasing scheme. *J. Atmos. Oceanic Technol.,* **18,** 1674–1683.

LeMone, M. A., and Coauthors, 2000: Land–atmosphere interaction research, early results, and opportunities in the Walnut River watershed in southeast Kansas: CASES and ABLE. *Bull. Amer. Meteor. Soc.,* **81,** 757–779.

Lhermitte, R. M., 1968: New developments in Doppler radar methods. Preprints, *13th Conf. on Radar Meteorology,* Montreal, QC, Canada, Amer. Meteor. Soc., 14–17.

Lugauer, M., and Coauthors, 2003: An overview of the VERTIKATOR project and results of alpine pumping. Preprints, *Int. Conf. on Alpine Meteorology,* Brigg, Switzerland, MeteoSwiss Publ. 66, 129–132.

Meischner, P., Ed., 2003: *Weather Radar: Principles and Advanced Applications.* Springer-Verlag, 300 pp.

Mohr, C. G., L. Miller, R. Vaughan, and H. Frank, 1986: The merger of mesoscale datasets into a common Cartesian format for efficient and systematic analysis. *J. Atmos. Oceanic Technol.,* **3,** 143–161.

Protat, A., and I. Zawadzki, 1999: A variational method for real-time retrieval of three-dimensional wind field from multiple-Doppler bistatic radar network data. *J. Atmos. Oceanic Technol.,* **16,** 432–449.

Quante, M., P. R. A. Brown, R. Baumann, B. Guillemet, and P. Hignett, 1996: Three aircraft intercomparisions of dynamical and thermodynamical measurements during the 'Pre-EUCREX' campaign. *Beitr. Phys. Atmos.,* **69,** 129–146.

Rogers, R. R., 1990: The early years of Doppler radar in meteorology. *Radar in Meteorology,* D. Atlas, Ed., Amer. Meteor. Soc., 122–129.

Satoh, S., and J. Wurman, 1999: Accuracy of composite wind fields derived from a bistatic multiple-Doppler radar network. Preprints, *29th Conf. on Radar Meteorology,* Montreal, QC, Canada, Amer. Meteor. Soc., 221–224.

——, and ——, 2003: Accuracy of wind fields observed by a bistatic Doppler radar network. *J. Atmos. Oceanic Technol.,* **20,** 1077–1091.

Schreiber, K.-J., 1998: Der Radarverbund des Deutschen Wetterdienstes. *Annalen der Meteorologie 38: Herbstschule Radarmeteorologie 1998,* Deutscher Wetterdienst, 47–65.

Schroth, A. C., M. S. Chandra, and P. Meischner, 1988: A C-band coherent polarimetric radar for precipitation and cloud physics research. *J. Atmos. Oceanic Technol.,* **5,** 803–822.

Stoelinga, M. T., P. V. Hobbs, C. F. Mass, J. D. Locatelli, N. A. Bond, B. A. Colle, J. R. A. Houze, and A. Rangno, 2003: Improvement of Microphysical Prameterization through Observational Verification Experiment (IMPROVE). *Bull. Amer. Meteor. Soc.,* **17,** 1807–1826.

Takaya, Y., and M. Nakazato, 2002: Error estimation of the synthesized two-dimensional horizontal velocity in a bistatic Doppler radar system. *J. Atmos. Oceanic Technol.,* **19,** 74–79.

WMO, cited 2002: Final report of expert team meeting on observational data requirements and redesign of the global observing system. [Available online at http://www.wmo.ch/web/www/reports.html.]

Wurman, J., 1994: Vector winds from a single-transmitter bistatic dual-Doppler radar network. *Bull. Amer. Meteor. Soc.,* **75,** 983–994.

——, S. Heckman, and D. Boccippio, 1993: A bistatic multiple-Doppler radar network. *J. Appl. Meteor.,* **32,** 1802–1814.

——, M. Randall, C. L. Frush, E. Loew, and C. L. Holloway, 1994: Design of a bistatic dual-Doppler radar for retrieving vector winds using one transmitter and a remote low-gain passive receiver. *Proc. IEEE, Special Issue on Remote Sensing Instruments for Environmental Research,* Vol. 82, 1861–1872.

Zrnić, D. S., 1996: Weather radar polarimetry—Trends toward operational applications. *Bull. Amer. Meteor. Soc.,* **77,** 1529–1534.